Vibration and dynamic loads in external gear pumps

Article *in* Archives of Civil and Mechanical Engineering · January 2015

Impact Factor: 1.79 · DOI: 10.1016/j.acme.2014.11.003

2 authors, including:

Wieslaw Fiebig

Wroclaw University of Science and Technol…

ACME-272; No. of Pages 9
ARTICLE IN PRESS
ARCHIVES OF CIVIL AND MECHANICAL ENGINEERING XXX (2015) XXX–XXX

Available online at www.sciencedirect.com
ScienceDirect
journal homepage: http://www.elsevier.com/locate/acme

Original Research Article

Vibration and dynamic loads in external gear pumps

W. Fiebig *, M. Korzyb

Wroclaw University of Technology, Faculty of Mechanical Engineering, ul. Łukasiewicza 7/9, 51-370 Wrocław, Poland

ARTICLE INFO

Article history:
Received 13 January 2014
Accepted 26 November 2014
Available online xxx

Keywords:
Gear pump modeling
Vibration
Dynamic loads
Simulation

ABSTRACT

This paper presents the model for simulation of vibration and dynamic loads in external gear pumps. The calculation has been carried out in Matlab/Simulink program. The vibrations of gears are excited due to the variable pressure forces and variable stiffness of the gearing. In this model the stiffness and damping coefficient of sliding bearings as well as the bending stiffness of gear wheels have been included. The influence of pressure and rotational speed on the dynamic forces in the bearings have been analyzed.

1. Introduction

External gear pumps are used in many applications, but their disadvantage is relatively high noise emission. As the causes of hydraulic noise generation are known, in particular, pressure and flow pulsation, trapped oil, pressure build-up and down and cavitation, most of these types of excitation can be largely compensated by various design measures [1,2]. Recent studies show that the pressure and flow pulsations are responsible for the noise and vibration generation in the hydraulic piping system, but not for the noise radiation of the pump itself. The intrinsic noise of the external gear pump is mainly dependent from the vibrations and dynamic loads on the gears [1]. These dynamic loads are transmitted through the bearings on the pump housing and cause vibrations and noise. In the paper the dynamical loads in an external gear pump have been evaluated by digital simulation of a dynamic model.

2. Vibration excitation forces on the gears

To analyze the dynamic processes in an external gear pump, the excitation forces, which are responsible for the vibration development of the gears, should be defined. Many papers are dealing with the definition of dynamic loads inside the sliding bearings of the gear pumps. The first approach has been published in 1990 [1], in which the excitation forces in the gear pump has been defined and the vibration model of the gearing has been described. The current papers regarding the dynamical behavior of gear pumps describe the flow and pressure distribution inside the gear pumps, excitations of gears due to the pressure and dynamical forces in the bearings are calculated [3]. These models include also the influence of the pressure ripples inside the pump, but as stated, this influence can be neglected at higher pressure.

* *Corresponding author*. Tel.: +48 609248046.
E-mail address: wieslaw.fiebig@pwr.edu.pl (W. Fiebig).
http://dx.doi.org/10.1016/j.acme.2014.11.003

Please cite this article in press as: W. Fiebig, M. Korzyb, Vibration and dynamic loads in external gear pumps, Archives of Civil and Mechanical Engineering (2015), http://dx.doi.org/10.1016/j.acme.2014.11.003

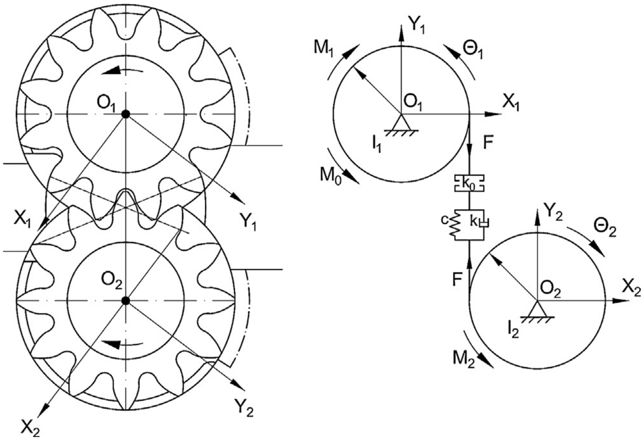

Fig. 1 – The dynamic model of the gearing [4–6].

In Fig. 1 the dynamic model of the gear pump shown in [4–6] has been described. This model includes the influence of the gearing on the reaction forces in the bearings.

2.1. *Torques on the gears due to the pressure*

The torque on the gears changes periodically depending on the position of the teeth contact point, which is sealing the delivery area from the suction area. In Fig. 2, two characteristic positions of this point have been shown at which the change of the torque as well as the radial forces on the gears occurs. In the range $0<\varphi\leq(\pi/z)\times(\varepsilon-1)$ the trapped volume is connected with the pressure chamber. In the other phase of the double teeth contact it is connected to the suction chamber; thus, the contact point S (Fig. 2a) of the preceding tooth pair (at the angle position $\varphi+(2\pi/z)$) is separating the pressure area from the suction area.

The pressure torque on the both gears can be calculated from:

$$M_1(\varphi)=\frac{p\times b}{2}\left[r_k^2-\rho_1^2\left(\varphi+\frac{2\pi}{z}\right)\right],\qquad M_2(\varphi)=\frac{p\times b}{2}\left[r_k^2-\rho_2^2\left(\varphi+\frac{2\pi}{z}\right)\right] \tag{1}$$

The distances between the contact point S and the middle point of the gears can be established from:

$$\begin{aligned}\rho_1^2(\varphi)&=r_k^2-2\times r_g\times\left(r_g\times\varphi-\frac{e}{2}\right)\times\sin\alpha_b+(r_g\times\varphi-e/2)^2\\ \rho_2^2(\varphi)&=r_k^2-2\times r_g\times\left(r_g\times\varphi-\frac{e}{2}\right)\times\sin\alpha_b+(r_g\times\varphi-e/2)^2\end{aligned} \tag{2}$$

After connecting the trapped volume with the suction chamber the contact point P separates the pressure chamber from the suction chamber (Fig. 2b). The torques due to the pressure in the angle range $(\pi/z)\times(\varepsilon-1)<\varphi\leq(2\pi/z)$ can be determined from:

$$M_1(\varphi)=\frac{p\times b}{2}[r_k^2-\rho_1^2(\varphi)],\qquad M_2(\varphi)=\frac{p\times b}{2}[r_k^2-\rho_2^2(\varphi)] \tag{3}$$

In Fig. 2, the calculated courses of torques have been shown ($t=\varphi/\omega$). From Fig. 2, it follows that the change of the position of the sealing point causes respectively the change in torque on both gears. The frequency of this change is equal to the gearing frequency and can be established from:

$$f_z=n\times\frac{z}{60} \tag{4}$$

The profile of the tooth normal force caused by the torque on the driven wheel is determined from:

$$F_{zn}(\varphi)=\frac{M_2(\varphi)}{r_g} \tag{5}$$

2.2. *Radial pressure loads on the gears*

The radial loads on the gears follow from the pressure distribution on its circumference. The experimental investigations confirm pressure distribution p (φ) shown in Fig. 3. One can distinguish three areas:

- the suction area (φ_1),
- the pressure build-up area and (φ_2),
- the pressure range of constant and variable proportion (φ_3), (φ_3'), share.

The size of each area depends on the design of the pump. For pumps without extending radial clearance compensation, the pressure build-up area φ_2 is spread on several teeth, unlike

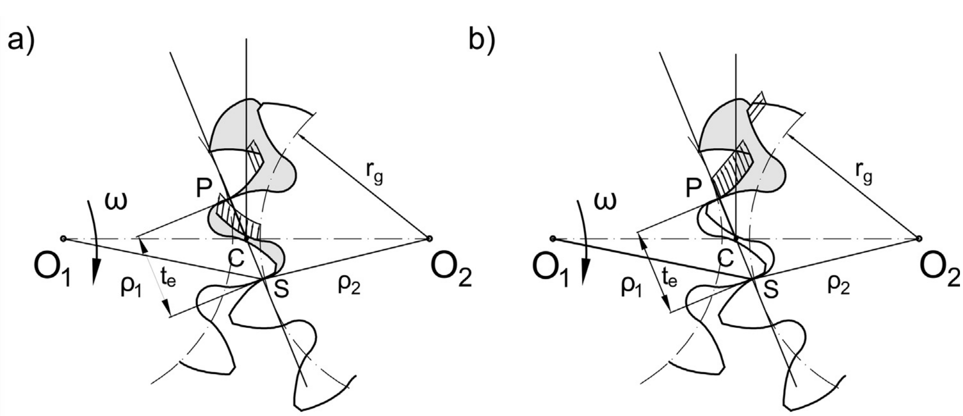

Fig. 2 – Scheme for the description of the torque changes.

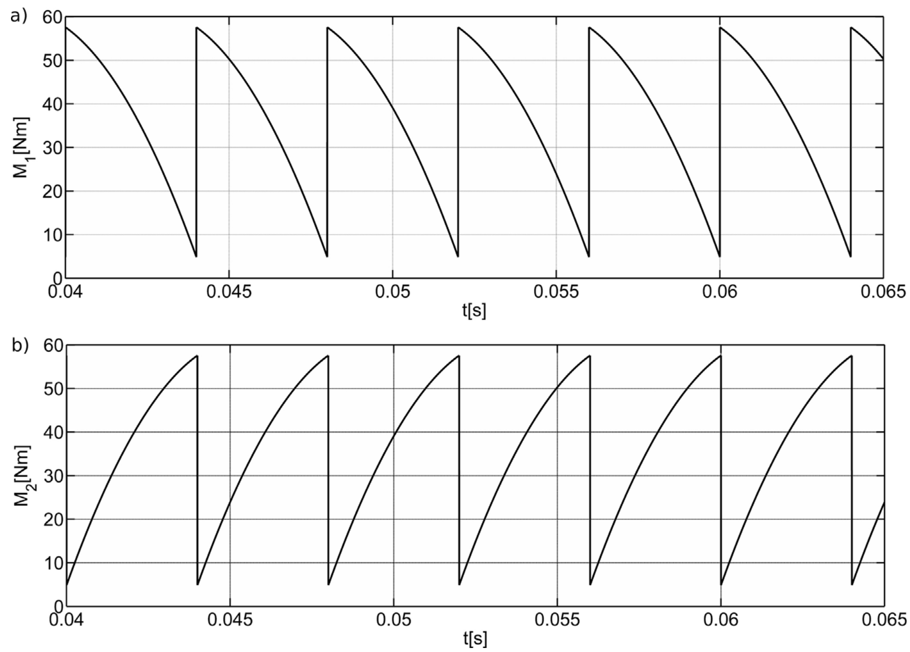

Fig. 3 – Torques on the gears in gear pump: (a) driving wheel and (b) driven wheel.

for pumps with radial clearance compensation. The size of the pressure build-up area also depends on the operating parameters of the pump [2]. In the calculation of the radial forces the size of areas φ_1 and φ_2 can be established based on the measured pressure distribution. The changes of the position of the sealing point cause periodic changes in the pressure in the range of φ_3'.

After the trapped volume is connected with the suction chamber, the sealing point changes its position from point S to P (Fig. 4), which causes a sudden change in the radial forces. The resulting radial forces are obtained by integrating over the circumference. The pressure forces on the driving and driven gear can be calculated from:

$$
\begin{aligned}
F_{hx1} &= -p \cdot b\left(r_a \cdot \sin\Phi_2 + \frac{t_e}{2}\cdot\cos\alpha_w\right)\\
F_{hy1} &= -p \cdot b\left(r_a \cdot \cos\Phi_2 + r_b - \frac{t_e}{2}\cdot\sin\alpha_w\right)\\
F_{hx2} &= -p \cdot b\left(r_a \cdot \sin\Phi_2 + \frac{t_e}{2}\cdot\cos\alpha_w\right)\\
F_{hy2} &= -p \cdot b\left(r_a \cdot \cos\Phi_2 + r_b - \frac{t_e}{2}\cdot\sin\alpha_w\right)
\end{aligned} \tag{6}
$$

In Fig. 5 the calculated time courses of the radial forces for both gears have been shown. The courses of the components of the pressure load in the x-direction are identical for both gears; however, they have an opposite sign. The change of the position of the sealing point leads to the change of forces.

2.3. *Excitations during the meshing of the gears*

Mechanical vibration excitation during the meshing of the gears in a gear pump is similar as in gear boxes and is resulting from [1,2]:

- time variable gearing stiffness as a result of the changing of the number of the engaged tooth pairs,
- disturbances during the gearing due to the manufacturing errors, for example pitch error and flank shape error.

During the meshing in a gear pump the teeth are deformed in an external gear due to the tooth contact force and in addition due to the unequal pressure forces on both tooth flanks in the gearing area. To determine the gearing stiffness along the line of action in a gear pump the method described in [2] has been used. In the area of the double tooth contact the

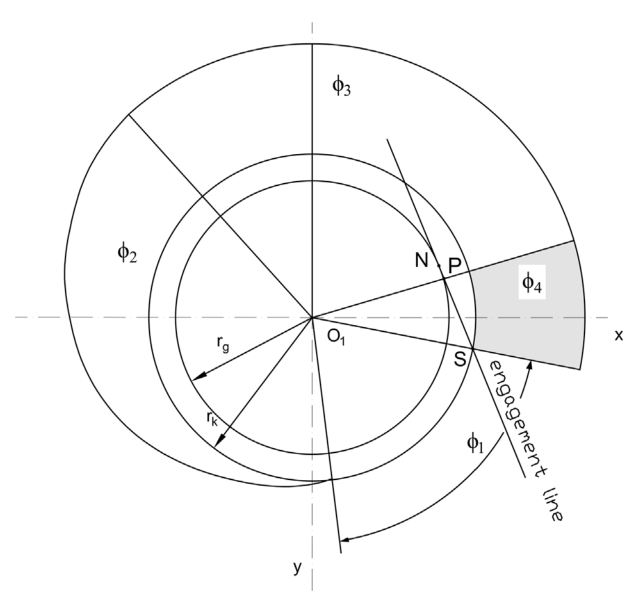

Fig. 4 – Pressure distribution on the gear circumference.

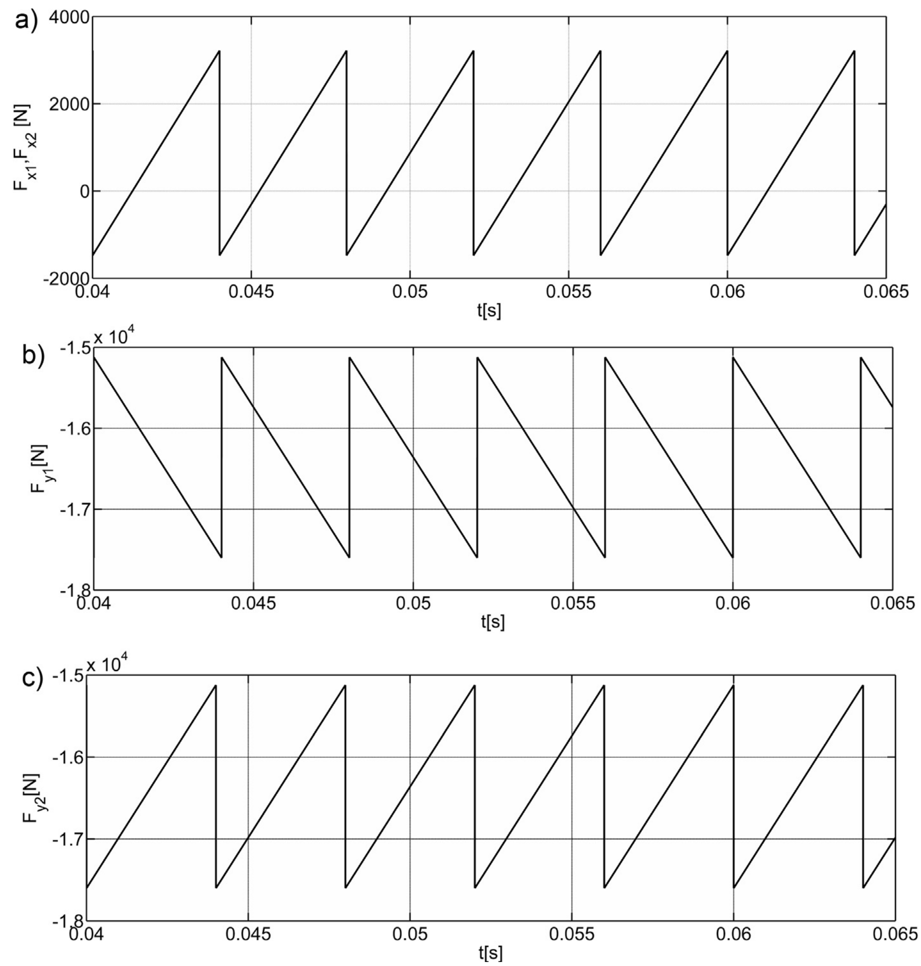

Fig. 5 – Variation of radial force components due to the pressure for $n = 1500\ min^{-1}$, $p = 20$ MPa: (a) in x-direction for both wheels, (b) in y-direction for driving wheel, and (c) in y-direction for driven wheel.

stiffness has been determined as the sum of the stiffness of individual tooth pairs. For the simulation model the trapezoidal changes of the gearing stiffness as in Fig. 6 has been considered.

3. Vibration model of a gear pump

The described excitations cause rotational and translational vibrations of the gears in the gear pump and these are coupled through the meshing. To investigate the influence of these excitation forces on the vibration of the gearwheels and dynamic loads in the external gear pumps the dynamic model shown in Fig. 7 has been considered.

The following simplifications have been assumed:

- the vibrations of the gears are considered at a constant angular velocity of the drive shaft,
- inertial forces of the oil inside the pump can be neglected,
- there is no pressure overdue in trapped volumes and the axial forces are compensated,
- there are no forces from unbalance on the gears,

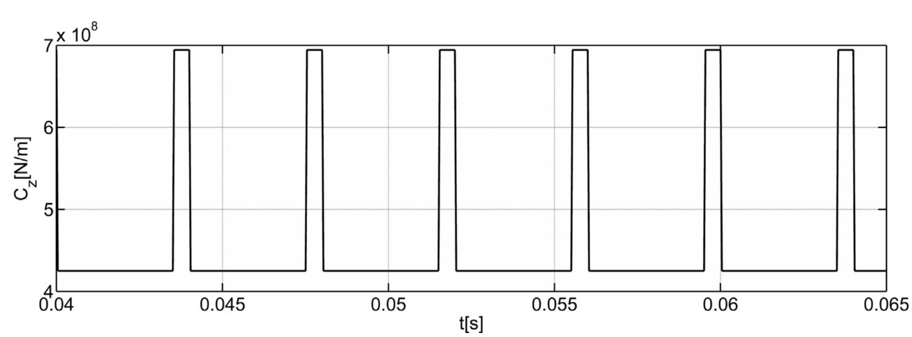

Fig. 6 – The change of the gearing stiffness along the line of action.

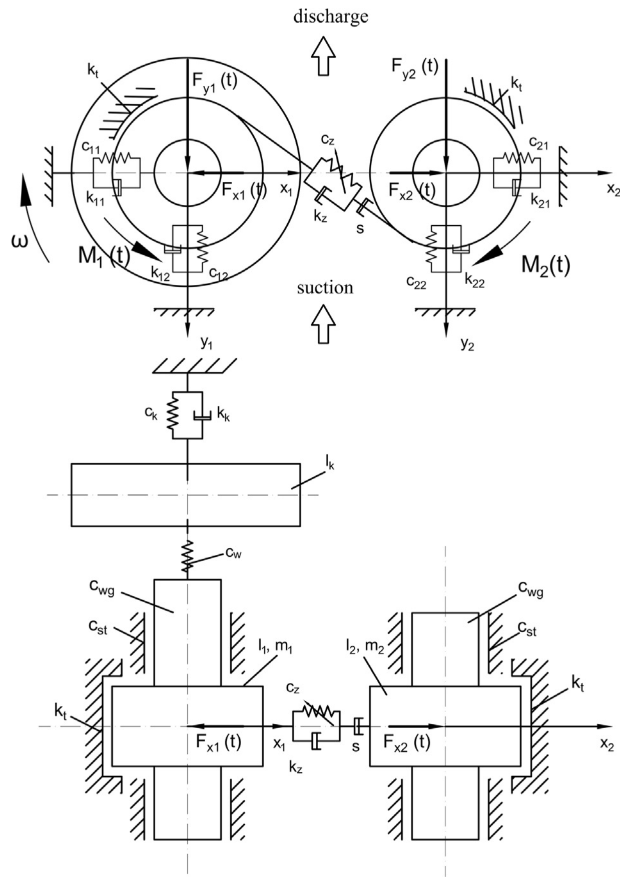

Fig. 7 – Dynamic model of an external gear pump.

- the manufacturing errors are negligibly small,
- the damping of torsional vibrations of the gears has a viscous character.

With the factor k_t the torsional damping due to oil in radial and axial gaps has been considered. It was assumed that the torque losses are equal for both gears and have a character of external damping.

There is also a possibility of direct transmission of the vibration energy from gears through the oil in radial gap to the pump housing. From investigations in [2] it is known that the transmission of the vibrational energy through this way is very small.

The gears are deflected toward the suction side due to pressure loads. These deflections are dependent on the bearing clearance and the deflection of the wheels. In Fig. 8 the displacements of the shaft center x_w, y_w from the static equilibrium position have been schematically shown. Absolute displacement of the shaft center $O_{stat}O_w$ is resulting from the shift due to the flexibility $O_{stat}O_{st}$ of the supporting housing, from the displacement due to the elasticity of the oil film in the bearings $O_{st}O_z$ and shaft deflection O_zO_w.

The stiffness of the sliding bearings at small oscillations around the static equilibrium position has been linearized with four stiffness and damping coefficients c_{ik}, b_{ik} ($i, k = 1, 2$). The stiffness and damping coefficients depend mainly on the load and geometry of the bearing, its clearance and the viscosity of the oil [1,2]. They were established using a computer program for bearings data of a pump (size 25).

For the components of the bearing forces the following equations are valid:

$$\begin{aligned} F_{Lxi} &= c_{11}(x_{zi}-x_{st}) + c_{12}(y_{zi}-y_{st}) + b_{11}(\dot{x}_{zi}-\dot{x}_{st}) + b_{12}(\dot{y}_{zi}-\dot{y}_{st}) \\ F_{Lyi} &= c_{21}(x_{zi}-x_{st}) + c_{22}(y_{zi}-y_{st}) + b_{21}(\dot{x}_{zi}-\dot{x}_{st}) + b_{22}(\dot{y}_{zi}-\dot{y}_{st}) \end{aligned} \tag{7}$$

(for $i = 1, 2$).

The displacements x_{st} and y_{st} in Eq. (7) can be established with FEM calculations for the pump housing. Starting from the equilibrium position, following differential equations for each degree of freedom can be written:

$$\begin{aligned} &I_k\ddot{\varphi}_k + c_k(\varphi_k - \omega t) + k_k(\dot{\varphi}_k - \omega) + c_w(\varphi_k - \varphi_1) = 0 \\ &I_1\ddot{\varphi}_1 + k_t\dot{\varphi}_1 - c_w(\varphi_k - \varphi_1) + F_n r_g \cos\alpha_b = -M_1(t) \\ &I_2\ddot{\varphi}_2 + k_t\dot{\varphi}_2 + F_n r_g \cos\alpha_b = -M_2(t) \\ &m_1\ddot{x}_{w1} + c_{wg}(x_{w1} - x_{z1}) + F_n \sin\alpha_b = -F_{x1}(t) \\ &m_2\ddot{x}_{w2} + c_{wg}(x_{w2} - x_{z2}) + F_n \sin\alpha_b = -F_{x2}(t) \\ &m_1\ddot{y}_{w1} + c_{wg}(y_{w1} - y_{z1}) + F_n \cos\alpha_b = -F_{y1}(t) \\ &m_2\ddot{y}_{w2} + c_{wg}(y_{w2} - y_{z2}) + F_n \cos\alpha_b = -F_{y2}(t) \\ &m_{z1}\ddot{x}_{z1} - \frac{1}{2}c_{wg}(x_{w1} - x_{z1}) + F_{Lx1} = 0 \\ &m_{z2}\ddot{x}_{z2} - \frac{1}{2}c_{wg}(x_{w2} - x_{z2}) + F_{Lx2} = 0 \\ &m_{z1}\ddot{y}_{z1} - \frac{1}{2}c_{wg}(y_{w1} - y_{z1}) + F_{Ly1} = 0 \\ &m_{z2}\ddot{y}_{z2} - \frac{1}{2}c_{wg}(y_{w2} - y_{z2}) + F_{Ly2} = 0 \end{aligned} \tag{8}$$

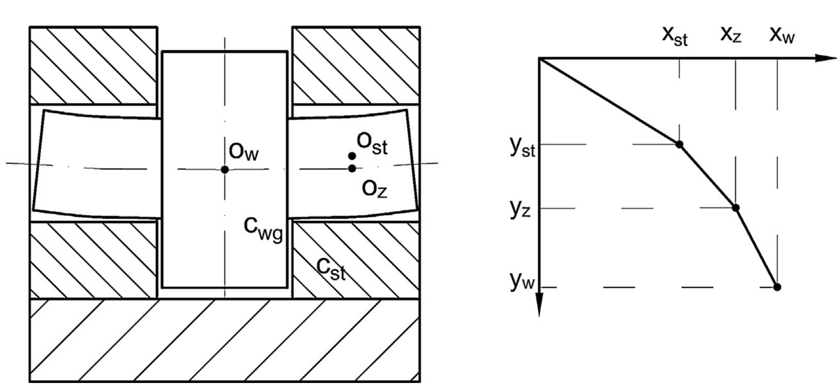

Fig. 8 – The decoupled deformation of the gear and its axial projection.

The dynamic force in the gearing along the line of action can be determined from:

$$F_n = \begin{aligned} & c_z(t)[(x_{w1} - x_{w2})\sin\alpha_b + (r_g\varphi_1 - r_g\varphi_2 + y_{w1} - y_{w2})\cos\alpha_b] \\ & + k_z[(\dot{x}_{w1} - \dot{x}_{w2})\sin\alpha_b + (r_g\dot{\varphi}_1 - r_g\dot{\varphi}_2 + \dot{y}_{w1} - \dot{y}_{w2})\cos\alpha_b] \end{aligned} \tag{9}$$

The dynamic torque on the pump shaft can be defined as:

$$M_d = c_w(\varphi_k - \varphi_1) \tag{10}$$

The equations of motion (8) have been solved using MATLab Simulink. For the calculations, the data of an external gear pump (size 25) with an axial gap compensation have been considered. Some of the parameters of the model such as mass moments of inertia J_k, J_1, J_2, torsional and bending stiffness of the pump shaft c_w, c_{wg} variable gearing stiffness $c_z(t)$ were determined by calculations. Other parameters such as torsional stiffness and damping factors of the coupling and c_k, k_k, or damping factor of gearing k_z have been assumed based on experimental studies. For the calculations at various operating parameters, the value of torsional damping factor in the radial gap k_t has been selected in a way that the calculated dynamic moment on the pump shaft is equal to the value of the experimentally determined average value.

Data for simulation	
Gear width	$b = 22.5$ mm
Number of teeth	$z = 10$
Module	$m = 4$ mm
Pressure angle	$\alpha_t = 27.81^\circ$
Tip radius of the gears	$r_k = 25$ mm
Moment of inertia of the clutch	$I_k = 2.22 \times 10^{-3}$ kg m^2
Moment of inertia of the driving gear	$I_1 = 18.00 \times 10^{-3}$ kg m^2
Moment of inertia of the driven gear	$I_2 = 13.10 \times 10^{-3}$ kg m^2
Damping factor of the clutch	$k_k = 2.02$ Nm s/rad
Torsional damping factor in the radial gap	$k_t = 0.08$ Nm s/rad
Damping factor in the gearing	$k_z = 4873$ Nm s/rad
Rotational stiffness of the clutch	$c_k = 1880$ Nm/rad
Bending stiffness of the gear shaft	$c_{wg} = 3.297 \times 10^9$ Nm/rad
Torsional stiffness of the pump shaft	$c_w = 29{,}868$ Nm/rad

4. Simulation results

The time courses of the dynamic moment on the pump shaft M_d, the dynamic contact force F_n and the components of dynamic bearing loads F_{Lxi}, F_{Lyi}, calculated on the basis of the model, are shown in Figs. 9 and 10. The fundamental changes of the dynamic loads in the pump come with the meshing frequency f_z. The changes with the frequency f_2 superimposed the changes with the frequency of f_z.

In Fig. 10 the dynamical reaction forces in the bearings at $n = 3000$ rpm have been shown.

Fig. 9b shows, that during the increasing of gearing stiffness (at the beginning of the double contact) it comes to a sudden increase of the dynamic gearing force. The vibrations are excited with the natural frequency of gearing and will decline due to the damping in the gearing. From the time courses of components of dynamic bearing forces F_{Lxi} and F_{Lyi} we can see, that due to the change of the excitation forces, the high frequency bending vibrations of the gear wheels have been excited. The amplitudes of these vibrations depend mainly on the amplitude of the harmonics of the excitation forces, the bending stiffnesses of the wheels and damping factors of the bearings. It follows also that the parametric changes of the gearing stiffness have a low impact on the dynamics of the gears.

5. Measurement results

The results of these measurements in terms of the dynamic moment on the pump shaft and the dynamic tooth load exhibit good agreement with the simulation results. In Fig. 11 the results of vibration measurements of a pump casing accordingly in x and y direction has been shown. It has been stated that for each period $T = 1/f_z$ the high frequency vibrations of the pump casing are excited. The appropriate records of the vibration velocity on the pump housing correspond to the calculated courses of bearing forces.

6. Summary

The paper presents a method for the analysis of the dynamic behavior of external gear pumps based on a dynamic model. The digital simulation of the model allows the investigation of individual influences of the pump operating and design parameters on the dynamical loads. The vibration excitations are caused by sudden position changes of the sealing point between pressure and suction zone in the gearing. The amplitude of the excitation force is directly dependent on the pressure. The dynamic loads in the bearings are determined by the bending vibrations of shafts as well as attenuation of the stiffness and damping in the bearings. The experimental investigations confirm the usefulness of the simulation model for the analysis of the dynamic behavior of external gear pumps. Optimization of pump parameters to reduce the vibrations and noise is possible on the basis of the model.

Nomenclature

b	gear width [m]
I_k, I_1, I_2	moments of inertia: the clutch, the driving wheel, the driven gear [kg m^2]
c_k, k_k	rotational stiffness and damping factor of the clutch [Nm/rad, Nm s/rad]
c_{st}	stiffness factor of the supporting body [Nm/rad]
c_{ik}, b_{ik}	stiffness and damping coefficients in sliding bearings [Nm/rad, Nm s/rad]
$c_z(t)$, k_z	variable gearing stiffness along the line of action and damping factor in the gearing [Nm/rad, Nm s/rad]
c_w, c_{wg}	torsional stiffness factor of the pump shaft and bending stiffness of the gear shaft [Nm/rad]
F_{xi}, F_{yi}	force components of gears as a result of the delivery pressure in the x- and y-direction [F]
F_n	dynamic tooth loading in the normal direction [F]

Please cite this article in press as: W. Fiebig, M. Korzyb, Vibration and dynamic loads in external gear pumps, Archives of Civil and Mechanical Engineering (2015), http://dx.doi.org/10.1016/j.acme.2014.11.003

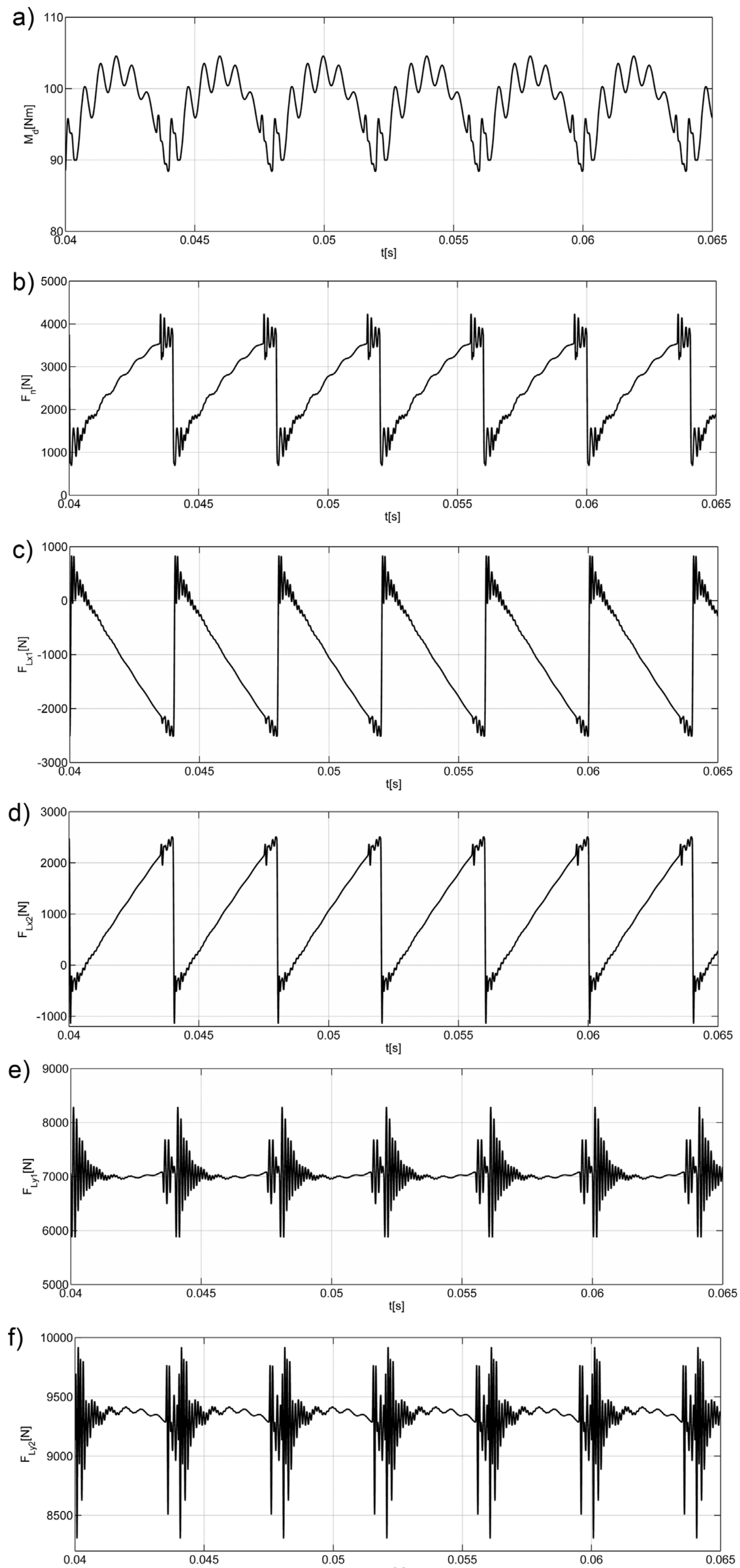

Fig. 9 – Calculated dynamic loads in an external gear pump at $n = 1500\ \mathrm{min}^{-1}$, $p = 20$ MPa: (a) dynamic moment on the pump shaft, (b) dynamic gearing force, (c and d) dynamic bearing forces in the x-direction, and (e and f) dynamic bearing forces in the y-direction.

k_t	torsional damping factor in the radial gap of the gears [Nm s/rad]
m_1, m_2	gear masses [kg]
m_{z1}, m_{z2}	shaft masses [kg]
$M_1(t)$, $M_2(t)$	variable torques on the gears as a result of the discharge pressure [Nm]
M_d	dynamic moment on the pump shaft [Nm]
r_k, r_b, r_g	tip, pitch and base radius of the gears [m]

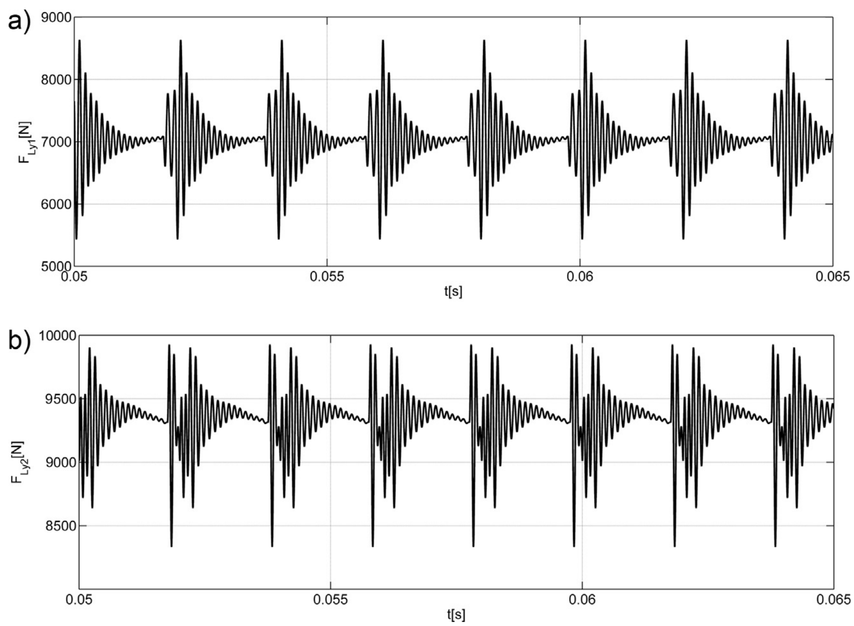

Fig. 10 – Calculated dynamic loads in an external gear pump at $n = 3000\ \text{min}^{-1}$, $p = 20$ MPa: (a) dynamic bearing force in the *y*-direction (driving gear) and (b) dynamic bearing force in the *y*-direction (driving gear).

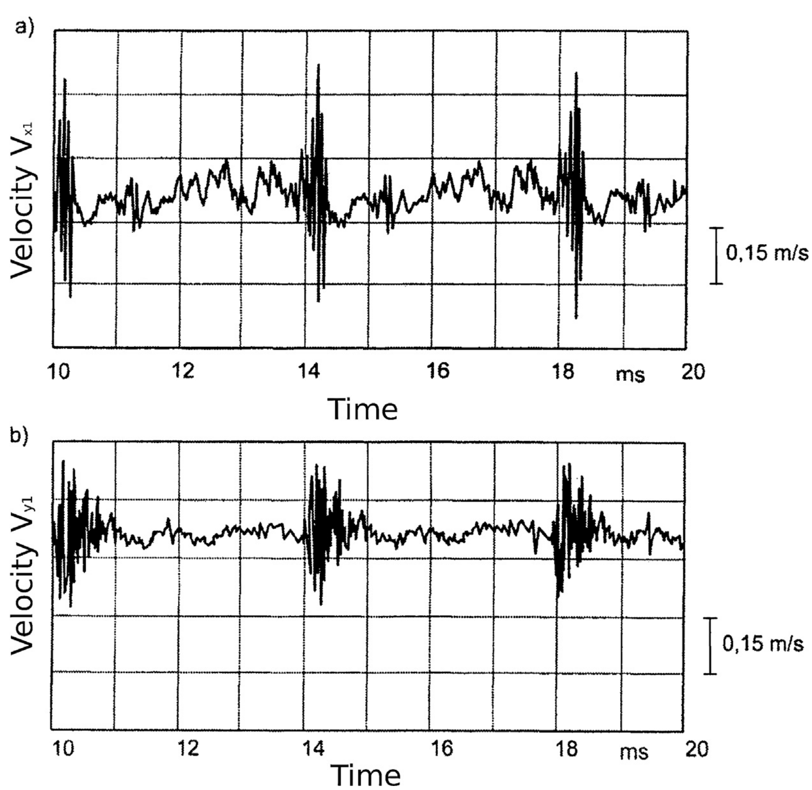

Fig. 11 – Measured time courses of the vibration velocity at the pump casing at $n = 1500\ \text{min}^{-1}$, $p = 20$ MPa: for the driving wheel in the (a) *x*- and (b) *y*-direction.

F_{Lxi}, F_{Lyi}	components of the bearing forces in x- and y-direction [N]
s	backlash [m]
t	time [s]
x_{wi}, x_{zi}	coordinates of displacement of the center of gears in x-direction [m]
y_{wi}, y_{zi}	coordinates of displacement of the center of gears in y-direction [m]
z	number of teeth

REFERENCES

[1] W. Fiebig, u. Heisel, Schwingungen und dynamische Belastungen in Außenzahnradpumpen; O+P; 34/1990.

[2] W. Fiebig, Schwingungs und Geraeuschverhalten der Verdraengerpumpen und hydraulischen Systeme, (Habilitationsschrift), University of Stuttgart, Germany, 2000, Oelhydraulik+Pneumatik O+P, No. 5 and 8, 1997.

[3] A. Vacca, M. Guidetti, Modeling and experimental validation of external spur gear machines for fluid power applications, Simulation Modelling Practice and Theory 19 (2011) 2007–2031.

[4] E. Mucchi, G. Dalpiaz, A. Fernandez del Rincón, Elastodynamic analysis of a gear pump. Part I: Pressure distribution and gear eccentricity, Mechanical Systems and Signal Processing 24 (2010) 2160–2179.

[5] E. Mucchi, G. Dalpiaz, A. Rivola, Elastodynamic analysis of a gear pump. Part II: Meshing phenomena and simulation results,, Mechanical Systems and Signal Processing 24 (2010) 2180–2197.

[6] L. Yulong, L. Kun, S. Fuchun, Dynamic model of gears with trapped oil and coupled analysis in external spur-gear pump, Applied Mechanics and Materials 130–134 (2012) 610–615.